Investigation on $Sr_{0.3}Ba_{0.7}Ce_{0.5}Zr_{0.35}Y_{0.1}Sm_{0.05}O_{3-\delta}$ perovskite for SOFC application

Nikdalila Radenahmad*, Ahmed Afif, Quentin Cheok,
Seikh Mohammad Habibur Rahman, Sten Eriksson, Abul Kalam Azad

***Abstract*—**Solid oxide fuel cell (SOFC) is attractive green energy resource since its promise in use of variety of fuels and low emission. Proton conducting materials enhanced conventional oxide conducting electrolyte has been achieving interest on its practicality in intermediate operating temperature. Combination of doped $BaCeO_3$ and $BaZrO_3$ with Sr, Y and Sm was studied as $Sr_{0.3}Ba_{0.7}Ce_{0.5}Zr_{0.35}Y_{0.1}Sm_{0.05}O_{3-\delta}$ (SBCZYSm). Rietveld refinement of the X-ray Diffractions (XRD) data reveals single phase material with cubic symmetry in the space group *Pm-3m*. Thermogravimetric Analysis (TGA) shows better stability on hydrated material in N_2 atmosphere compared to dried sample. SBCZYSm performs high conductivity in wet Argon condition. Scanning Electron Microscopy (SEM) shows that the material is highly densed with the density about 6.06 g/cm^3. Particle size was also studied and reveal average diameter of 5.8 µm approximately.

***Keywords*—**Proton conductor, solid oxide fuel cell electrolyte, Rietveld refinement, conductivity.

I. INTRODUCTION

Solid oxide fuel cell (SOFC) is an alternative choice to produce green energy since its low emission and feasibility in variety of fuels[1]. The most generally studied oxide ion conducting electrolyte for SOFC is yttria-stabilized zirconia (YSZ) that operates at high temperature in range of 800 °C – 1000 °C. Since the high operating temperature involves heat generation that requires the higher expense, lower operating temperature in intermediate temperature solid oxide fuel cells (IT-SOFCs) has got attraction to reduce the heat consumption. Proton conducting electrolytes show the successful operation at 400 – 700 °C to overcome the operating temperature problem[2],[3]. By this intermediate temperature range, several perovskite electrolytes (general formula, ABO_3) perform good electrochemical properties in term of proton conductivity[4]. Although typical oxide ion conductor is used widely in SOFC, the difficulties are still presence in terms of mismatched materials, low tolerance in operating conditions and fuel efficiencies. Oxide ion conductor enhanced by proton conducting material shows promise to improve the operating performances. Report reveals the higher efficiency of proton conducting solid oxide fuel cell (SOFC-H^+) than oxide ion conducting solid oxide fuel cell (SOFC-O^{2-}) at intermediate temperature range (400 – 700 °C). However, its maximum voltage and power density are still lower than oxide ion conducting electrolytes e.g. YSZ[5]. The doped $BaCeO_3$ is one of the best proton conductors but it is unstable in CO_2 and H_2O surrounding atmosphere. Although $BaZrO_3$ shows lower conductivity than $BaCeO_3$, it performs the stability under CO_2 and steam atmosphere, particularly 10 mol % Y doped $BaZrO_3$. By these properties, combination of doped $BaCeO_3$ and $BaZrO_3$ has got interest on their high proton conductivity and good stability in humid atmosphere[5],[6]. Several dopants have been studied in order to improve stability and conductivity. Most of the reports have done on doping some percentage of Ce and/or Zr that was substituted by tri-valent cations like Y, Yb, Sc, Pr, Sm etc. This doping at the B-site makes oxygen vacancies to enhance the conductivity[7]-[12]. For example, Ce was doped by Zr to increase proton conductivity and chemical stability as the study on $BaCe_{0.9-x}Zr_xY_{0.1}O_{2.95}$ series which show good chemical stability in steam and carbon dioxide atmospheres[9],[10]. Y doping reveals potential to enhance conductivity in conventional materials of $BaZrO_3$ and $BaCeO_3$. Y doped $BaZrO_3$ exhibits high conductivity of 7.38 mS/cm at 650 °C[13]. Amount of Ce at B-site has strong effect on proton concentration in perovskite materials[14]. Fei He et al.[15] showed the potential on $BaCe_{0.5}Zr_{0.3}Y_{0.2}O_{3-\delta}$ electrolyte as its high dense. Sm-doped proton conductors exhibits promising performance for IT-SOFCs[16]. Since $SrZrO_3$ and $SrCeO_3$ based electrolyte are also widely studied as proton conductors, Sr is attractive doped element to Ba at A site to study the behavior in terms of structure and electrochemical properties[17],[18]. Only some works study on Ba substitution by Sr or Ca which can also improve protonic conductivity[19].

In this study, Ce and Zr were doped by Y and Sm at the B-site and substituted Ba by Sr to examine the structural and electrochemical performance. A new perovskite material, $Sr_{0.3}Ba_{0.7}Ce_{0.5}Zr_{0.35}Y_{0.1}Sm_{0.05}O_{3-\delta}$, was prepared and characterized. This shows promising results for future study and applications.

*Nikdalila Radenahmad is with Faculty of Integrated Technologies, Universiti Brunei Darussalam, Gadong, Brunei Darussalam (corresponding author's phone: +6738900398; e-mail: 14m0507@ubd.edu.bn).

Ahmed Afif is with Faculty of Integrated Technologies, Universiti Brunei Darussalam, Gadong, Brunei Darussalam (e-mail: 14m0506@ubd.edu.bn).

Quentin Cheok is with Faculty of Integrated Technologies, Universiti Brunei Darussalam, Gadong, Brunei Darussalam (e-mail: hoonnam.cheok@ubd.edu.bn).

Seikh Mohammad Habibur Rahman is with Department of Chemistry and Chemical Engineering, Chalmers University of Technology, Gothenburg, Sweden (e-mail: habibur@chalmers.se).

Sten Eriksson is with Department of Chemistry and Chemical Engineering, Chalmers University of Technology, Gothenburg, Sweden (e-mail: stene@chalmers.se).

Abul Kalam Azad is with Faculty of Integrated Technologies, Universiti Brunei Darussalam, Gadong, Brunei Darussalam and Centre for Advanced Materials and Energy Studies, Universiti Brunei Darussalam, Gadong, Brunei Darussalam (e-mail: abul.azad@ubd.edu.bn).

II. Experimental

$Sr_{0.3}Ba_{0.7}Ce_{0.5}Zr_{0.35}Y_{0.1}Sm_{0.05}O_{3-\delta}$ was prepared by solid state reaction method. Proportional amount of SrO, $BaCO_3$, CeO_2, ZrO_2, Y_2O_3 and Sm_2O_3 powders were mixed with ethanol and grinded by agate mortar and pestle. The mixture was sintered in air at 950 °C for 8 hours. Hydraulic press was used to make 13 mm diameter pallets by pressing at 4 psi and sintered at 1400 °C and 1450 °C for 6 hours and 8 hours, respectively. X-ray diffraction (XRD) analysis was carried out by a reflection type Shimadzu-7000 diffractometer (λ=1.5406 Å) in the 2θ range from 10° to 80° in air. Rietveld refinement was performed using FullProf software[20]. Scanning electron microscopy (SEM) was performed using a Phenom ProX electron microscope to study the structural morphology and crystalline size. The sintered pallets were coated by Pt in a sputtering device of Quorom Q150RS to make the conducting surface. Pt paste was painted on 13 mm diameter pallet and sintered at 1000 °C for 2 hours. Impedance spectroscopy was carried out by using Solartron 1260 impedance analyzer in the frequency range of 100 mHz - 6 MHz and 1 V rms in signal amplitude in the temperature range 1000 °C to 150 °C with step of 50°C. This experiment was operated in wet Argon atmosphere (Ar flowing through water at room temperature). Impedance data was analyzed by Z-View software (Scribner Associates Inc.) to find conductivity. The hydreated samples were prepared in hydration furnace by 0.4 P_{N_2} at 800 °C, 600 °C, 400 °C, 200 °C and 150 °C by dwelling for 2 h, 2 h, 48 h, 2 h and 55 h, respectively. The heating and cooling rate was 200 °C/hour until 400 °C and 10 °C/hour for cooling down to 150 °C. This hydration purpose is to examine chemical and thermal stability and proton intake capacity by using a NETZSCH Thermogravimetric Analyzer (TGA). It was operated under 20 ml/min constant flow of nitrogen. Particle size analysis was carried out after manual grinding by agate mortar and pestle for 10-15 minutes using HORIBA particle size analyzer.

III. Results and Discussion

Sintered material was studied by X-ray diffraction analysis to identify crystal structure. Fig. 1 shows the XRD pattern of $Sr_{0.3}Ba_{0.7}Ce_{0.5}Zr_{0.35}Y_{0.1}Sm_{0.05}O_{3-\delta}$. Indexing of the pattern was performed using the software TREOR90 and subsequent refinement of cell parameters were performed by using Checkcell. Indexing of the pattern shows crystallization in the cubic symmetry.

Rietveld analysis of the XRD data confirms that the material crystallize in the cubic symmetry in the space group of Pm-3m(No. 227). Rietveld refinement profile of $Sr_{0.3}Ba_{0.7}Ce_{0.5}Zr_{0.35}Y_{0.1}Sm_{0.05}O_{3-\delta}$ was shown in Fig. 2. The refinement result shows the unit cell parameter of 4.288() Å, unit cell volume of 78.82(1) $Å^3$ and χ^2 of 1.11.

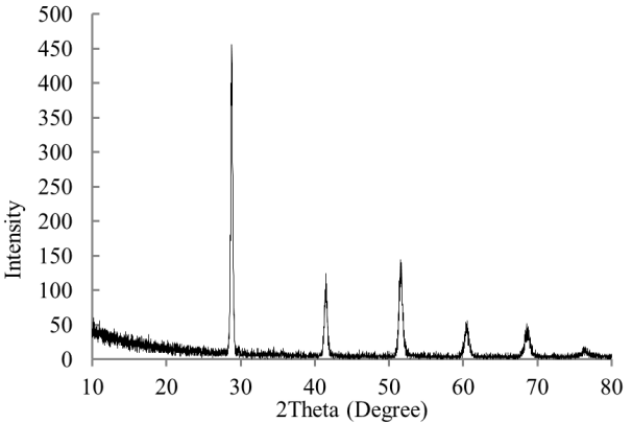

Fig. 1 X-Ray diffraction pattern for SBCZYSm

The lattice parameters is comparable to typical perovskite based materials $BaCeO_3$ (a = 4.445 Å)[21] and $BaZrO_3$ (a = 4.193 Å)[22]. The phase structure of $BaCeO_3$-$BaZrO_3$ is highly dependent on the concentration Ce/Zr at the B-site. Typically, Y-doped $BaCeO_3$ is orthorhombic and Y-doped $BaZrO_3$ is cubic. In fact, symmetry and cell parameters can be different in multiple doped $BaCeO_3$ depending on their B-site cation ratios, synthesis route and final sintering temperature.

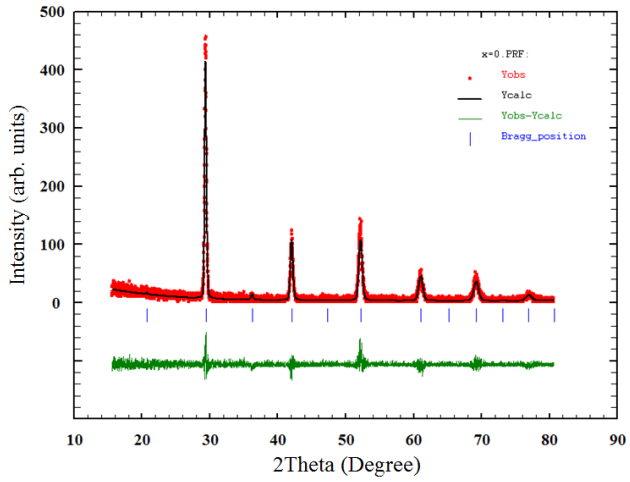

Fig. 2 Rietveld refinement profile

$BaCe_{0.9-x}Zr_xY_{0.1}O_{3-\delta}$ shows orthorhombic structure for x = 0.1 and 0.2 while cubic structure is on x ≥0.3[11]. When the Y percentage is little bit more in $BaCe_{0.8-x}Zr_xY_{0.2}O_{3-\delta}$, the phase structure is orthorhombic for x = 0.1 - 0.5 and cubic when x = 0.6 - 0.8 [10]. Sm and Y doped $BaCeO_3$ also shows orthorhombic crystal structure[16]. However, $Sr_{0.3}Ba_{0.7}Ce_{0.5}Zr_{0.35}Y_{0.1}Sm_{0.05}O_{3-\delta}$ exhibits cubic symmetry due to its high concentration of Ce. These studies reveal the influence of the preparation procedure and sintering temperatures involved for obtaining the materials onto their crystalline structures. Higher calcination temperature, normally used for solid state reaction, might have important effect in changing the symmetry in the crystal structure that displays in sharper pattern.

The density of the material was calculated using the unit cell volume obtained from Rietveld refinement in the formula,

$$D = \frac{Z \times F.W.}{V \times Na} \quad (1)$$

Where D is the density, Z is no. of formula unit, F.W. is the formula weight, V is the unit cell volume and Na is Avogadro's number. Refinement shows the density on SBCZTSm of 6.06 g/cm^3

Dried and hydrated sample were examined to compare performances on the thermal behavior by thermogravimetric analysis from 20 °C to 1000 °C. Fig. 3 reveals the TGA plot of $Sr_{0.3}Ba_{0.7}Ce_{0.5}Zr_{0.35}Y_{0.1}Sm_{0.05}O_{3-\delta}$.

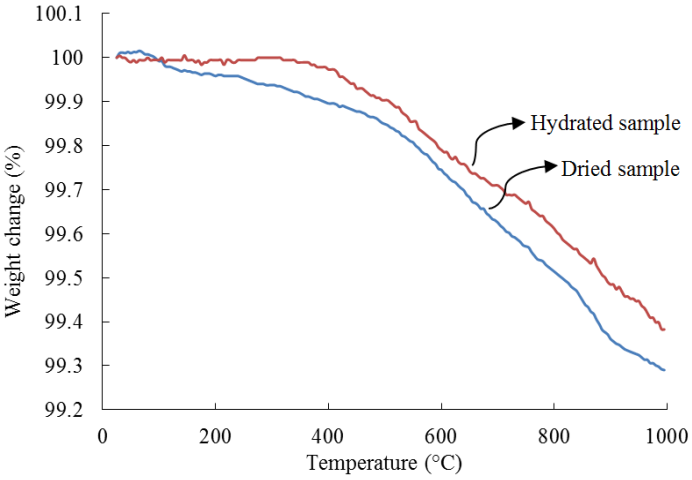

Fig. 3 Mass change on dried and hydrated sample

On dried sample, mass slightly gained at the beginning due to adsorbtion of gas and subsequent lost 0.151 % until reach the decomposition temperature, 500 °C. The decomposition point influence mass loss dramatically. In contrast for hydrated sample, mass is stable until severe loss around 400 °C. These indicates losing of proton that was absorbed during the hydration process in the atomic structure on making the O-H bond. Hydrated sample shows better thermal stability until 400 °C compared to dried sample. The location of protons in the structure can be observed from neutron diffraction experiments[23],[24].

Micro-scale features play important role in fuel cell electrolytes that need to be gas tight to prevent the mixing of gaseous reactants. In proton conducting oxides, grain boundary resistance is detrimental to total conductivity. An increase in grain size can reduce number of grain boundaries, which obviously results in reduction of grain boundary resistance. This effects total ionic conductivity increases but may make it weaker. Fig. 4 shows the SEM images of the morphology of the $Sr_{0.3}Ba_{0.7}Ce_{0.5}Zr_{0.35}Y_{0.1}Sm_{0.05}O_{3-\delta}$ pallet surface sintered at 1450 °C for 8 hours. The grain size lies between 1-2 µm approximately.

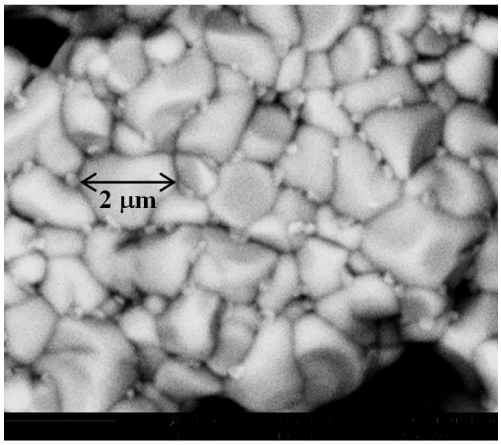

Fig. 4 Morphology on SEM image

For this material, grain was well defined and density was high as observed from the images which show potential in applying as electrolyte for SOFCs.

Fig. 5 shows the Arrhenius plot of the total ionic conductivity of $Sr_{0.3}Ba_{0.7}Ce_{0.5}Zr_{0.35}Y_{0.1}Sm_{0.05}O_{3-\delta}$ pellet under wet Ar atmosphere in the temperature range 250 – 700 °C.

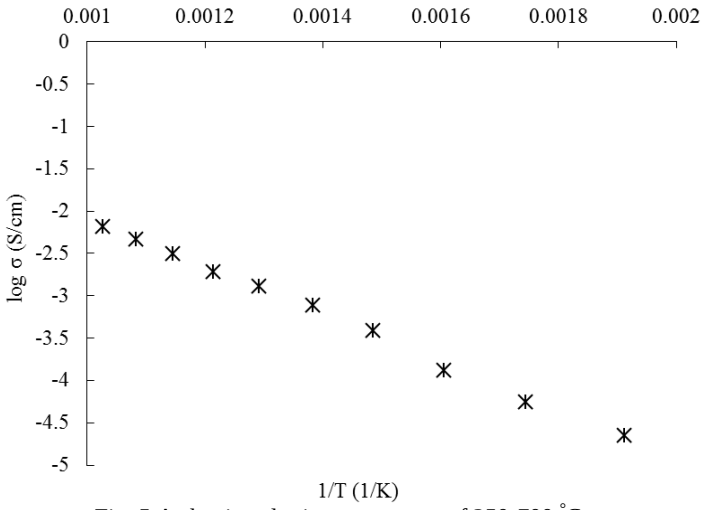

Fig. 5 Arrhenius plot in temperature of 250-700 °C

At 700 °C, the conductivity was 6.42 x 10^{-3} S/cm with activation energy of 0.5659 eV.

At high temperatures, protons in proton conducting perovskites are supposed to follow Grotthuss mechanism[25], [26] and transport in the following steps: i) a proton associated with a fixed oxygen atom; ii) the proton-oxygen bond reorients under the influence of the neighboring oxygen atoms; finally iii) the proton starts to oscillate between the two oxygen atoms and eventually moves to the neighboring oxygen[5]. The binding energy between $OH^{\bullet}$ and $M_{B'}$ varies with the dopant. Simulation results shows that the binding energies of $OH^{\bullet}$ - $M_{B'}$ (hydroxyl – dopant pairs at the nearest neighbor sites) for Y, Yb and In were -0.26, -0.35 and -0.58 eV, respectively which has good agreement with the experimental results[27]. A more stable state for hydroxyl-dopant pair will be found for a more negative value of the binding energies.

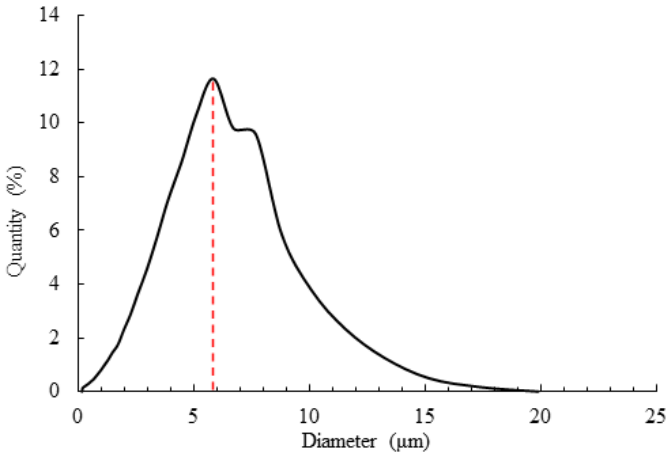

Fig. 6 Particle size distribution for SBCZYSm

Particle size of $Sr_{0.3}Ba_{0.7}Ce_{0.5}Zr_{0.35}Y_{0.1}Sm_{0.05}O_{3-\delta}$ was shown in Fig. 6. The analysis was carried out after grinding the sample with agate mortar and pestle for 10-15 minutes. The particle size has great quantity in 4.5-8.5 μm and the diameter of maximum quantity is nearly 5.8 μm. However, the particle size of material is expected to be controlled from preparing by ball milling method to reduce porosity of material which is the requirement of being electrolytes.

IV. Conclusions

This work is on proton conducting perovskite material in order to utilize as electrolyte in SOFC particularly in intermediate temperature. $Sr_{0.3}Ba_{0.7}Ce_{0.5}Zr_{0.35}Y_{0.1}Sm_{0.05}O_{3-\delta}$ was investigated as possible electrolyte. Rietveld refinement of XRD data reveals cubic symmetry in the *Pm-3m* space group. Thermal behavior on hydrated material performs better stability up to 400 °C compared to dried material. SEM image exhibit grain size of 1-2 μm and is characterized as dense material. Doped material shows advantage in high conductivity as 6.42 x 10^{-3} S/cm at 700 °C with activation energy of 0.566 eV. Characterizations of invisible features are significant to identify the structure of material which require researcher to develop materials direct to use in fuel cell as green energy.

Acknowledgment

We are grateful to Center for Advanced Materials and Energy Science (CAMES) and Applied Physics Program, UBD for their cooperation in some of the experiments. The authors, NR and AA would like to thank Ministry of Foreign Affairs and Trade (MOFAT) for giving the scholarship to do research in the Universiti Brunei Darussalam. NR is also grateful to Professor Sten Eriksson to manage a summer scholarship to perform this work at Chalmers University of Technology, Sweden.

References

[1] N. Q. Minh, "Ceramic Fuel Cells," *J. Am. Ceram. Soc.*, vol. 76, no. 3, pp. 563–588, 1993.

[2] S. Tao and J. T. S. Irvine, "A stable, easily sintered proton-conducting oxide electrolyte for moderate-temperature fuel cells and electrolyzers," *Adv. Mater.*, vol. 18, no. 12, pp. 1581–1584, 2006.

[3] E. Fabbri, D. Pergolesi, and E. Traversa, "Materials challenges toward proton-conducting oxide fuel cells: a critical review," *Chem. Soc. Rev.*, vol. 39, no. 11, pp. 4355–4369, 2010.

[4] D. Medvedev, A. Murashkina, E. Pikalova, A. Demin, A. Podias, and P. Tsiakaras, "$BaCeO_3$: Materials development, properties and application," *Prog. Mater. Sci.*, vol. 60, pp. 72–129, Mar. 2014.

[5] Z. Shi, W. Sun, and W. Liu, "Synthesis and characterization of $BaZr_{0.3}Ce_{0.5}Y_{0.2-x}Yb_xO_{3-\delta}$ proton conductor for solid oxide fuel cells," *J. Power Sources*, vol. 245, pp. 953–957, Jan. 2014.

[6] A. AZAD and J. IRVINE, "Synthesis, chemical stability and proton conductivity of the perovksites $Ba(Ce,Zr)_{1-x}$ Sc_x $O_{3-\delta}$," *Solid State Ionics*, vol. 178, no. 7–10, pp. 635–640, Apr. 2007.

[7] A. K. Azad and J. T. S. Irvine, "High density and low temperature sintered proton conductor $BaCe_{0.5}Zr_{0.35}Sc_{0.1}Zn_{0.05}O_{3-\delta}$," *Solid State Ionics*, vol. 179, no. 19–20, pp. 678–682, 2008.

[8] Z. Tao, Z. Zhu, H. Wang, and W. Liu, "A stable $BaCeO_3$-based proton conductor for intermediate-temperature solid oxide fuel cells," *J. Power Sources*, vol. 195, no. 11, pp. 3481–3484, Jun. 2010.

[9] L. Yang, S. Wang, K. Blinn, M. Liu, Z. Liu, Z. Cheng, and M. Liu, "Enhanced sulfur and coking tolerance of a mixed ion conductor for SOFCs: $BaZr_{0.1}Ce_{0.7}Y_{0.2-x}Yb_xO_{3-\delta}$," *Science*, vol. 326, no. 5949, pp. 126–129, 2009.

[10] E. FABBRI, A. DEPIFANIO, E. DIBARTOLOMEO, S. LICOCCIA, and E. TRAVERSA, "Tailoring the chemical stability of $Ba(Ce_{0.8-x}Zr_x)Y_{0.2}O_{3-\delta}$ protonic conductors for Intermediate Temperature Solid Oxide Fuel Cells (IT-SOFCs)," *Solid State Ionics*, vol. 179, no. 15–16, pp. 558–564, Jun. 2008.

[11] K. Katahira, Y. Kohchi, T. Shimura, and H. Iwahara, "Protonic conduction in Zr-substituted $BaCeO_3$," *Solid State Ionics*, vol. 138, no. 1–2, pp. 91–98, 2000.

[12] Y. Liu, L. Yang, M. Liu, Z. Tang, and M. Liu, "Enhanced sinterability of $BaZr_{0.1}Ce_{0.7}Y_{0.1}Yb_{0.1}O_{3-\delta}$ by addition of nickel oxide," *J. Power Sources*, vol. 196, no. 23, pp. 9980–9984, 2011.

[13] J. Li, J. L. Luo, K. T. Chuang, and A. R. Sanger, "Chemical stability of Y-doped $Ba(Ce,Zr)O_3$ perovskites in H_2S-containing H_2," *Electrochim. Acta*, vol. 53, no. 10, pp. 3701–3707, 2008.

[14] S. Ricote, N. Bonanos, and G. Caboche, "Water vapour solubility and conductivity study of the proton conductor $BaCe_{(0.9-x)}Zr_xY_{0.1}O_{(3-\delta)}$," *Solid State Ionics*, vol. 180, no. 14–16, pp. 990–997, 2009.

[15] F. He, D. Song, R. Peng, G. Meng, and S. Yang, "Electrode performance and analysis of reversible solid oxide fuel cells with proton conducting electrolyte of $BaCe_{0.5}Zr_{0.3}Y_{0.2}O_{3-\delta}$," *J. Power Sources*, vol. 195, no. 11, pp. 3359–3364, Jun. 2010.

[16] Z. Shi, W. Sun, Z. Wang, J. Qian, and W. Liu, "Samarium and Yttrium Codoped BaCeO3 Proton Conductor with Improved Sinterability and Higher Electrical Conductivity," *ACS Appl. Mater. Interfaces*, vol. 6, no. 7, pp. 5175–82, 2014.

[17] T. SAKAI, S. MATSUSHITA, H. MATSUMOTO, S. OKADA, S. HASHIMOTO, and T. ISHIHARA, "Intermediate temperature steam electrolysis using strontium zirconate-based protonic conductors," *Int. J. Hydrogen Energy*, vol. 34, no. 1, pp. 56–63, Jan. 2009.

[18] T. Sakai, H. Matsumoto, T. Kudo, R. Yamamoto, E. Niwa, S. Okada, S. Hashimoto, K. Sasaki, and T. Ishihara, "High performance of electroless-plated platinum electrode for electrochemical hydrogen pumps using strontium-zirconate-based proton conductors," *Electrochim. Acta*, vol. 53, no. 28, pp. 8172–8177, Nov. 2008.

[19] I.-M. Hung, H.-W. Peng, S.-L. Zheng, C.-P. Lin, and J.-S. Wu, "Phase stability and conductivity of $Ba_{1-y}Sr_yCe_{1-x}Y_xO_{3-\delta}$ solid oxide fuel cell electrolyte," *J. Power Sources*, vol. 193, no. 1, pp. 155–159, 2009.

[20] J. Rodriguez-Carvajal, "Recent advances in magnetic structure determination by neutron powder diffraction + FullProf," *Phys. B Condens. Matter*, vol. 192, no. 1–2, p. Pages–55, 1993.

[21] J. Wu, R. A. Davies, M. S. Islam, and S. M. Haile, "Atomistic study of doped $BaCeO_3$: Dopant site-selectivity and cation nonstoichiometry," *Chem. Mater.*, vol. 17, no. 4, pp. 846–851, 2005.

[22] R. L. Moreira and A. Dias, "Comment on 'Prediction of lattice constant in cubic perovskites,'" *J. Phys. Chem. Solids*, vol. 68, no. 8, pp. 1617–1622, 2007.

[23] A. K. Azad and J. T. S. Irvine, "Location of Deuterium Positions in the Proton-Conducting Perovskite $BaCe_{0.4}Zr_{0.4}Sc_{0.2}O_{2.90}$ x D_2O by Neutron Powder Diffraction," *Chem. Mater.*, vol. 21, no. 2, pp. 215–222, 2008.

[24] I. Ahmed, C. S. Knee, M. Karlsson, S.-G. Eriksson, P. F. Henry, A. Matic, D. Engberg, and L. Börjesson, "Location of deuteron sites in the proton conducting perovskite $BaZr_{0.50}In_{0.50}O_{3-y}$," *J. Alloys Compd.*, vol. 450, no. 1–2, pp. 103–110, 2008.

[25] N. Agmon, "The Grotthuss mechanism," *Chemical Physics Letters*, vol. 244, no. 5–6. pp. 456–462, 1995.

[26] D. Marx, "Proton transfer 200 years after Von Grotthuss: Insights from ab initio simulations," *ChemPhysChem*, vol. 7, no. 9. pp. 1849–1870, 2006.

[27] M. S. Islam, P. R. Slater, J. R. Tolchard, and T. Dinges, "Doping and defect association in $AZrO_3$ (A = Ca,Ba) and $LaMO_3$ (M = Sc,Ga) perovskite-type ionic conductors," *Dalt. Trans.*, no. 19, pp. 3061–3066, 2004.